Biosensors and Bioelectronics 136 (2019) 132–139

Contents lists available at ScienceDirect

Biosensors and Bioelectronics

journal homepage: www.elsevier.com/locate/bios

Point-of-care genetic analysis for multiplex pathogenic bacteria on a fully integrated centrifugal microdevice with a large-volume sample

Hau Van Nguyen, Van Dan Nguyen, Eun Yeol Lee, Tae Seok Seo*

Department of Chemical Engineering, Kyung Hee University, Yongin, 17104, South Korea

ARTICLE INFO

Keywords:
Centrifugal microdevice
Portable genetic analyzer
Loop-mediated isothermal amplification
Colorimetric detection
Super absorbent polymer
Food-borne bacteria

ABSTRACT

We present a fully integrated portable centrifugal microsystem for multiplex detection of food poisoning bacteria with a large volume of sample up to 1 mL. The microsystem consists of a portable genetic analyzer and a fully integrated centrifugal microdevice. The centrifugal microdevice is designed with two units: a 3D printed solution-loading cartridge and a centrifugal microfluidic disc. All the essential solutions for loop-mediated isothermal amplification (LAMP) reaction are stored inside the cartridge, and orderly released into centrifugal microdevice by a rotation program. Each unit of the device is designed with 20 reaction chambers for simultaneous detection of food-borne bacteria in one test. To increase the amount of a sample to 1 mL, we incorporated the super absorbent polymer (SAP) in the waste chamber to absorb the sample and the washing solution during the device operation. The whole process was automatically conducted including designated solution release, bead-based DNA extraction, isothermal gene amplification by Eriochrome Black (EBT)-mediated LAMP reaction, and colorimetric and UV–visible detection of amplicons. The ratio between Abs_{640nm} and Abs_{570nm} was used as a criterion to confirm the positive result, and the result was positive upon the condition of $Abs_{640}/Abs_{570} \geq 1.0$. To demonstrate the pathogenic bacteria detection on our proposed microsystem, we targeted three kinds of bacteria (*Escherichia coli* O157:H7, *Salmonella typhimurium*, and *Vibrio parahaemolyticus*) for monoplex and multiplex detection. The whole process from sample to result was completed within 1 h with a low limit of detection (LOD) of 10^2 cells/mL.

1. Introduction

Point-of-care testing (POCT) is recently blooming up and plays a vital role in supporting immediate treatment. The central laboratories are equipped with high cost and automatic diagnostic platform for highly sensitive, precise and accurate analysis. However, due to the bulkiness of the analytical instruments, they are not adequate for on-site diagnostics. On the contrary, the POCT allows simple and rapid analysis, which can help the doctor to make a timely decision on the treatment for patients. In addition, the POCT offers a user-friendly prototype suitable for the un-trained worker, full integration and automatic operation for fast analysis, minimizing human interferences for sample storage and transportation to eliminate contamination issues, and cost-effectiveness adequate for resource-limited environments.

The POCT system includes a paper-based microfluidic device (Choi et al., 2015, 2017a,; Ye et al., 2018), a lateral flow assay (Choi et al., 2017a,b; Deng et al., 2018; Takalkar et al., 2017), a microfluidic device (DuVall et al., 2017; Zhang et al., 2017), a smartphone-based device (Berg et al., 2015; Priye et al., 2016; Stedtfeld et al., 2012; Wang et al., 2017). Among them, a microfluidic device has attracted huge attention over decades, and a centrifugal microfluidic device has advanced remarkably as a promising candidate for complex diagnostic purposes. Centrifugal microfluidics have demonstrated high fidelity for the unit operation and integration on a single device such as sample loading and reagent storage (Hoffmann et al., 2010; Stumpf et al., 2016; van Oordt et al., 2013; Zhao et al., 2017), serial dilution (Kim et al., 2018), metering, aliquoting, mixing, incubation (Choi et al., 2016; Jung et al., 2015; Oh et al., 2016a,b; Park et al., 2017), and detection (Andreasen et al., 2015; Martin et al., 2017; Schwemmer et al., 2016).

Although the integrated centrifugal microfluidics have proven a number of biological applications such as immunoassay and genetic analysis, the major challenge of the integrated centifugal microdevice for POCT is the solution treatment of a large volume of sample, which can eventually affect the LOD of the assay (Antillon et al., 2018; Loonen et al., 2013). Because the intrinsic volume of the microfluidic dimension ranges from nanoliter to microliter, it is not easy to incorporate high volume of the sample in the fully integrated centrifugal microdevice. For example, Zhao et al. showed an enzyme-linked

* Corresponding author.
E-mail address: seots@khu.ac.kr (T.S. Seo).

https://doi.org/10.1016/j.bios.2019.04.035
Received 25 January 2019; Received in revised form 18 March 2019; Accepted 17 April 2019
Available online 20 April 2019
0956-5663/

immunosorbent assay (ELISA) to detect C-reactive protein in the centrifugal device with a sample volume of 50 µL (Zhao et al., 2017). Liu et al. performed the real-time reverse transcription LAMP on a centrifugal device to detect avian influenza virus with a sample volume of 40 µL (Liu et al., 2018). Choi et al. reported the real-time LAMP for Malaria detection with a sample volume of 180 µL (Choi et al., 2018). Till now, the fully integrated centrifugal disc has been developed to operate with a relatively low volume of sample, which needs high concentration of the target pathogen in the sample to achieve a reliable result. Considering that a small number of pathogens could be fatal (Antillon et al., 2018), a pre-enrichment step for a large volume of the sample is crucial, especially for diluted pathogen samples.

In this study, we propose a fully integrated POC centrifugal microsystem, which is capable of treatment for a large volume of the sample (up to 1 mL) to identify multiplex pathogen bacteria (*Escherichia coli* O157: H7, *Vibrio parahaemolyticus*, and *Salmonella enterica subsp.*). The integrated centrifugal microfluidic disc is combined with the sample loading cartridge for automatic operation, and executes the bead-based DNA extraction, the isothermal amplification by an EBT-mediated LAMP reaction, and the amplicon detection by a UV–vis detector in a sequential order. In addition, we constructed a portable genetic analyzer which is equipped with a motor, a heater, and a UV–vis detector to demonstrate the sample-to-answer capability of POC DNA testing.

2. Materials and methods

2.1. Design and fabrication of the integrated centrifugal microdevice

The centrifugal disc (Dia. 13 cm) was designed with two units on a single device (Fig. 1a). Each unit consists of the solid-phase DNA extraction part and the multiplex LAMP assay part. Four reservoirs (for a sample solution, a washing solution, an elution solution, and a LAMP cocktail) were patterned, which were linked with a 3D printed sample loading cartridge (see below). The bead bed channel is connected with the sample injection hole, and acid-treated silica beads are packed in the zigzag shaped channel. A delay chamber is placed after the washing solution reservoir to confirm the sequential loading of the sample solution and then the washing solution. In the waste chamber, the SAP is incorporated to absorb the sample and washing solution. In the collection chamber, the LAMP cocktail and the elution solution with purified genomic DNA are collected, and then are aliquoted into reaction chambers.

The centrifugal microdevice was designed with AutoCAD (Autodesk, USA), and etched in a 3.0 mm thick poly(methylmethacrylate) (PMMA) plate (Acrytal, Korea) using a CNC machine (Tinyrobo, Korea). All the siphon channels were coated with a hydrophobic reagent, Vistex 111-50 (FSI Coating Technologies, USA). The reaction chamber was coated with primer sets of the target bacteria. The waste chamber was integrated with SAP from baby diaper (Pamper, USA) for utterly absorbing 1 mL of a sample solution. A pressure sensitive adhesive (PSA) foil layer (no. 900360, HJ-BIOANALYTIK GmbH, Germany) was applied to seal the disc. The acid-washed glass beads (150-212 µm, Sigma, USA) were then packed into the zigzag channel. Finally, the bead-packed channel was incubated in 6M Gu-HCl for 30 min to enhance the DNA capture capacity (Fig. 1c). The digital image of the device is shown in Fig. 1b.

2.2. Design and fabrication of the sample loading cartridge

For the automatic solution loading into the device, a 3D-printed cartridge is fabricated which has rooms for the sample solution, the washing solution, the elution solution, and the LAMP cocktail (Fig. 2a). Each solution can be ejected separately depending on the RPM. The volume for each solution is 1 mL for a sample, 50 µL for a washing

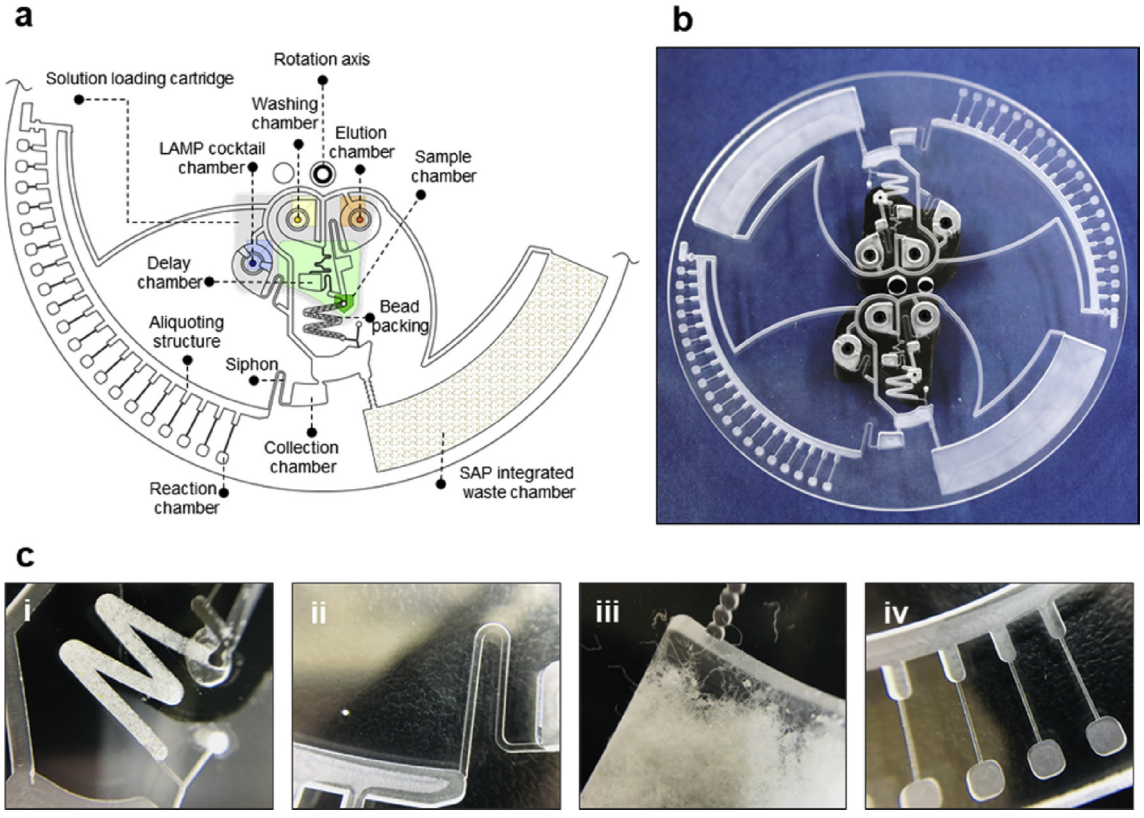

Fig. 1. (a) Schematic illustration of the integrated centrifugal disc. (b) A digital image of the disc. (c) Components of the centrifugal microdevice. (i) A glass bead-packed microchannel for DNA extraction, (ii) a siphon channel coated with Vistex, (iii) a SAP incorporated waste chamber, and (iv) aliquoting structure and the LAMP reaction chambers.

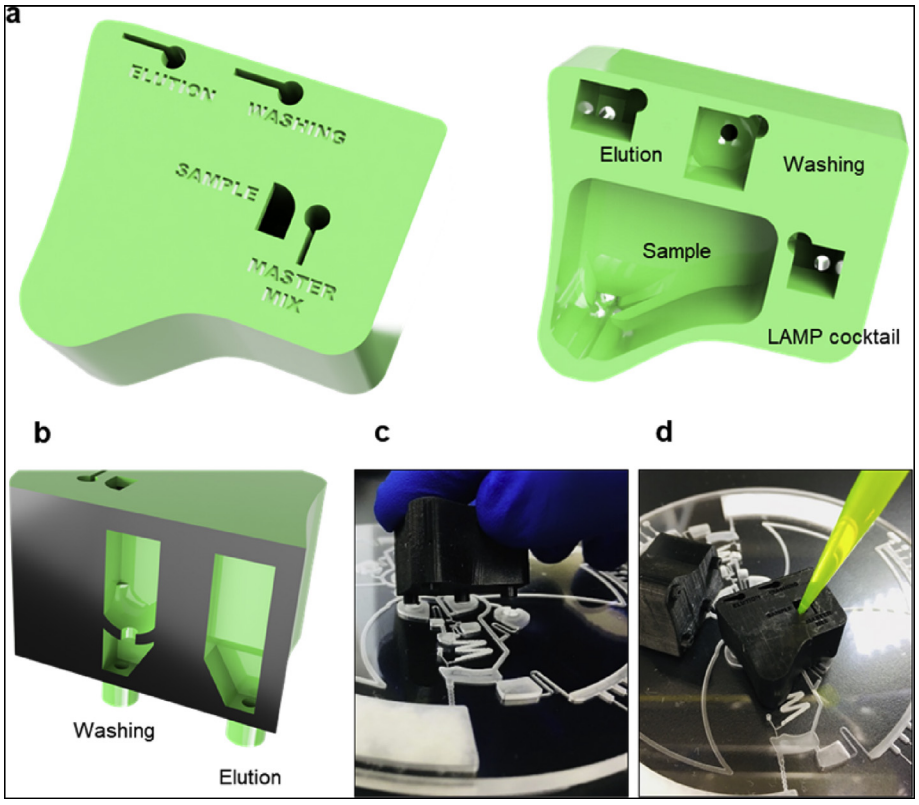

Fig. 2. (a) Design of the 3D printed solution loading cartridge with internal chambers for containing the sample, elution, washing, and LAMP cocktail solution (top and bottom view). (b) Design of the washing chamber with double rooms, and the elution chamber with a single room. (c) Attachment of the sample loading cartridge on the centrifugal microdevice. (d) Injection of the solution into the cartridge through the injection hole.

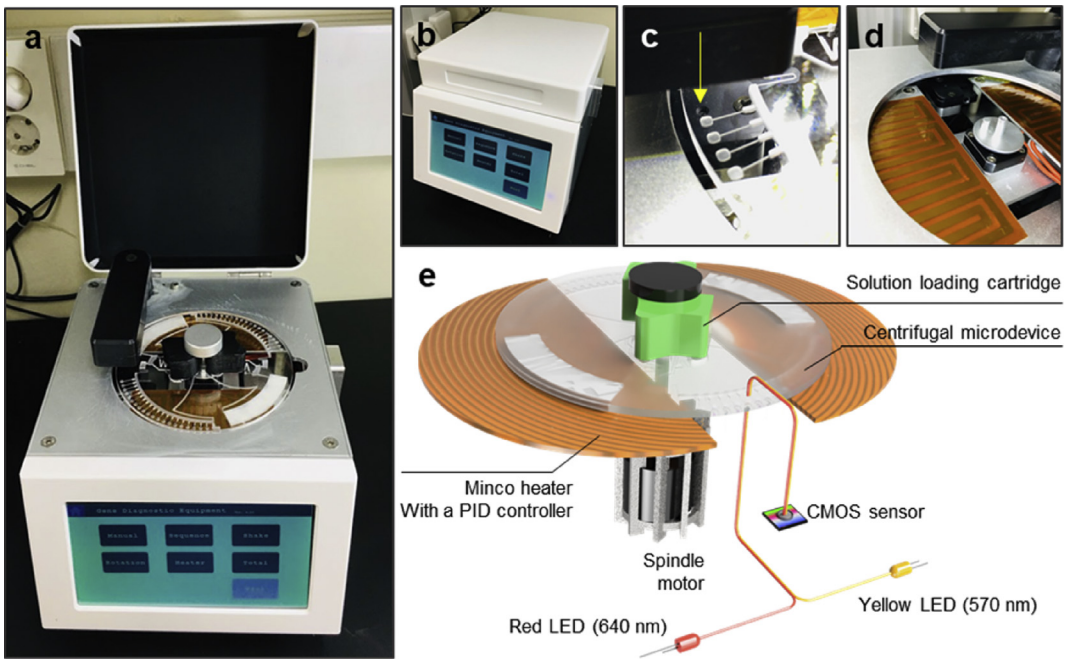

Fig. 3. (a, b) Digital images of the portable genetic analyzer. (c) A couple of Minco heaters. (d) A UV–vis detector for measuring the absorbance of the reaction chamber. (e) Schematic illustration of the integrated genetic analyzer platform with a motor, a couple of Minco heaters, and a UV–vis detector with two LED light sources at 640 and 570 nm.

solution, 50 μL for an elution solution, and 50 μL for a LAMP cocktail. The cartridge was designed with a Fusion360 program (Autodesk, USA) and was fabricated using a DLP 3D printer (Cubicon, Korea). The material of the cartridge is ABS-like resin (Cubicon, Korea), and the dimensions is 3.0 cm [length] × 2.6 cm [width] × 1.7 cm [height].

2.3. Portable genetic analyzer

For the POC DNA testing, we constructed a portable and compact genetic analyzer for operating the integrated centrifugal microdevice. The platform consists of (1) a spindle motor (Maxon, Switzerland), (2) a couple of Minco heaters and (3) a UV–visible optical detector. The whole real image of the portable genetic analyzer combined with the

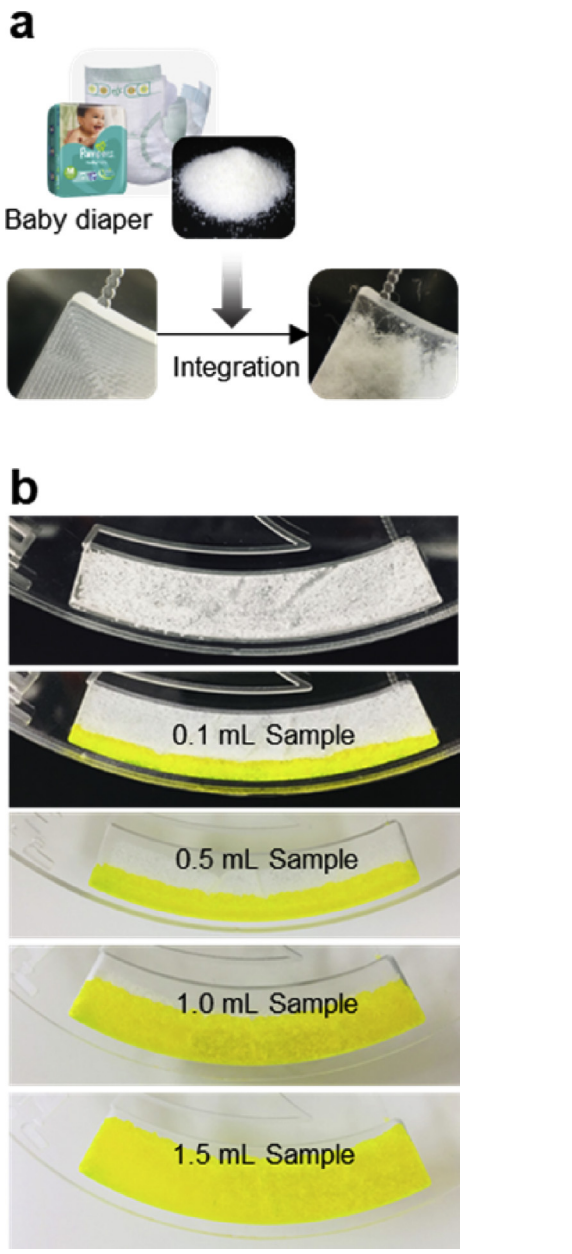

Fig. 4. (a) A super absorption polymer (SAP) integrated waste chamber. (b) Testing SAP absorption capacity with the various volume of sample ranging from 0.1 mL to 1.5 mL.

centrifugal device is shown in Fig. 3a. The front side is the LCD panel in which we can touch the screen to input the experimental protocol. The total size of the genetic analyzer is 20 cm [length] × 22 cm [width] × 20 cm [height] (Fig. 3b). Fig. 3c displays the Minco heaters. The ramping rate of the heater is 0.43 °C/s for heating and 0.09 °C/s for natural cooling. For UV–visible absorbance detection, a yellow LED 570 nm and a red LED 650 nm (Roithner Lasertechnik GmbH, Austria) are used and positioned toward the LAMP reaction chamber through an optical fiber (Fig. 3d). A filter (Thorlabs, England) and an aspheric lens (Thorlabs, England) were employed for eliminating the interference from the excited light and for reducing optical aberrations, respectively. The transmittance light intensity as then measured by a CMOS camera sensor (Basler, Germany) and converted into the absorbance ratio of Abs_{640}/Abs_{570} (Fig. 3e).

2.4. Preparation of bacterial samples

Escherichia coli O157: H7 (KCCM 11835), *Vibrio parahaemolyticus* (KCCM 11965), and *Salmonella enterica subsp.* enterica serotype Typhimurium (KCCM 11806) were purchased from Korean Culture Center of Microorganisms (Korea). According to the manufacturers' instructions, those bacteria were cultured in designated media. The cultured bacteria were rinsed three times with DNase/RNase water (Thermo Fisher Scientific, USA) and diluted into various concentrations ranging from 2×10^2 cells/mL to 2×10^5 cells/mL for the further experiment.

2.5. Preparation of LAMP reagents

The primer sets for targeting three bacteria were designed by PrimerExplorerV5 software (Eiken Chemical Co., Tokyo, Japan) and provided by Macrogen (Korea). Information of target genes and primer sequences is shown in Table S1. To prepare LAMP cocktails, Bst 2.0 WarmStart DNA Polymerase, 10 mM dNTP, and Eriochrome Black T (EBT) were purchased from New England Biolabs (USA), Bioneer (Korea) and Sigma (USA), respectively. The volume of the individual reaction chamber is 4 μL, which is composed of 12 mM Tris-HCl, 30 mM KCl, 4.0 mM $MgSO_4$, 6.0 mM $(NH_4)_2SO_4$, 0.06% Tween 20, 3 mM dNTPs, 0.8 U μL^{-1} Bst 2.0 WarmStart DNA Polymerase, 6.4 μM FIP, 6.4 μM BIP, 0.8 μM F3, 0.8 μM B3, and 60 μM EBT. The temperature for the LAMP reaction was 63 °C, and the success of the LAMP reaction was confirmed by a colorimetric detection mediated by EBT and UV–vis absorption spectrometry.

2.6. Procedure for the on-chip genetic analysis in a portable genetic analyzer

Firstly, 1 mL of the lysed sample was prepared containing 500 μL of a bacteria sample solution, 250 μL of an AL buffer (Qiagen, Netherlands), and 250 μL of 6 M Gu-HCl (Thermo Fisher Scientific, USA). The sample solution, the washing solution (70% ethanol), the elution solution (DNase/RNase water), and the LAMP/EBT cocktail solution were then injected into the cartridge through the injection hole (Fig. 2d). An in-house program automatically performed all the operation steps including spinning for transferring solutions, shaking for mixing, heating for proceeding the LAMP reaction, measuring the real-time UV–vis absorbance of the reaction chamber, and reporting data.

3. Results and discussion

3.1. Design of the centrifugal microdevice with integration of SAP for a large volume of sample processing

Fig. 1 shows the schematics of the centrifugal microdevice having four solution reservoirs (a lysed sample solution, a washing solution, an elution, and a LAMP/EBT cocktail), a bead packed microchannel, a delay chamber, 20 reaction chambers, and a waste chamber with SAP. The sample solution, the washing solution, and the elution solution was orderly released into the bead-packed channel by a sophisticated microfluidic design and a simple RPM control. Genomic DNA in the lysed sample solution was first bound on the glass bead surface, and the contaminants were washed out with the washing solution. The washing solution was delayed in an appropriate time, and flushed into the bead-packed channel later than the sample solution due to the delay chamber. After solid phase extraction in the bead-packed channel (Jung et al., 2013; Oh et al., 2016a,b), the bound bacteria genomic DNA was eluted to the collection chamber together with the LAMP/EBT cocktail and then divided into 20 aliquots by a metering structure. The aliquots were injected into each reaction chamber with high speed and the LAMP reaction was proceeded for identifying multiplex food poisoning bacteria in parallel.

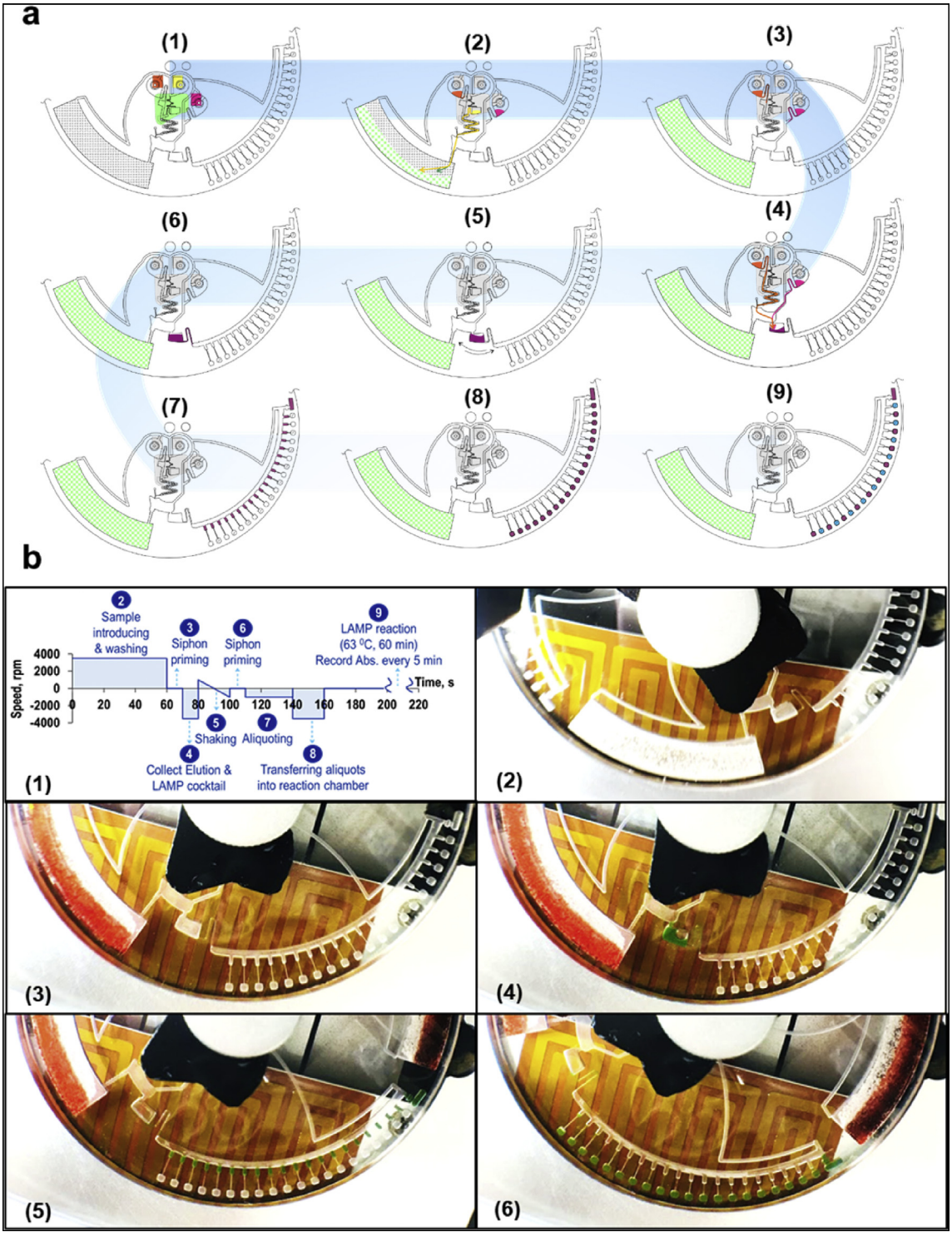

Fig. 5. (a) The overall schematics for the chip operation. (b) The rotation profile and representative real images of the chip operation.

For automatic sample loading into the device, we designed the sample loading cartridge with a 3D printing technology as shown in Fig. 2. In the cartridge, four rooms were patterned in which four essential solutions for the LAMP reaction (a lysed sample solution, a washing solution, an elution, and a LAMP/EBT cocktail) were stored inside (Fig. 2a). In particular, the volume of the sample was 1 mL for pretreatment of a large volume of sample. The design of these chambers produces a capillary force higher than gravity to prevent bleeding of the solutions.

However, the wettability of the washing solution (70% ethanol) was so high, leading to leakage of the washing solution from the cartridge into the device before running the spinning program. Therefore, we designed a specific double chamber structure for a washing solution container (Fig. 2b). The washing solution was initially stayed in the upper chamber, and then moved to the lower chamber gently to minimize the downward pressure. The outlet of the cartridge was matched to the reservoir holes and clicked to the device (Fig. 2c). The four solutions were injected into the cartridge through the injection hole (Fig. 2d) and then orderly released into the centrifugal device by a spinning program.

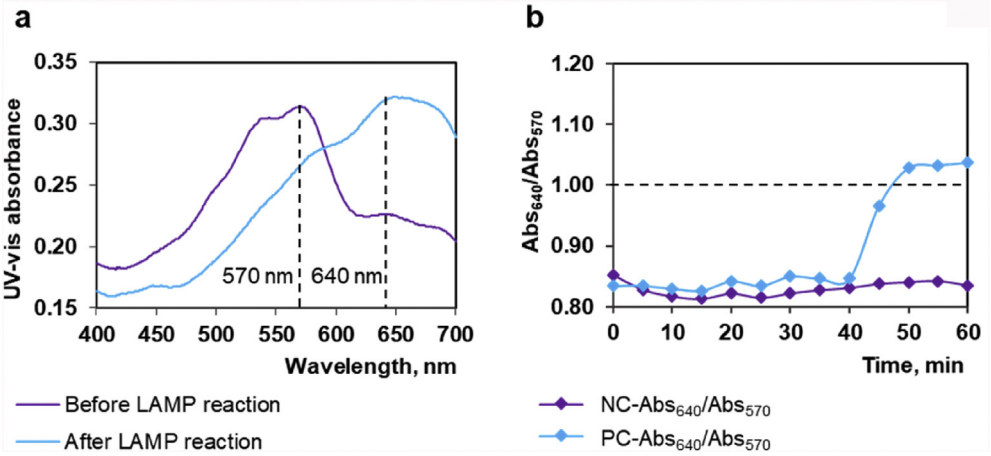

Fig. 6. (a) UV–vis absorption spectra of the LAMP mixture before and after the LAMP reaction by a commercial UV–vis spectrophotometer. (b) Real-time profile of Abs_{640}/Abs_{570} of the NC and PC by the proposed portable genetic analyzer system.

For treating 1 mL of a sample solution, we incorporated SAP in the waste chamber. The SAP was obtained from a baby diaper, and 0.2 g of the SAP was attached in the waste chamber by using a double adhesive tape (Fig. 4a). Various volume of the sample solution ranging from 0.1 mL to 1.5 mL was tested to validate the absorption capacity of the integrated SAP chamber.

As shown in Fig. 4b, we achieved a high absorption capacity up to 1.5 mL of a sample solution without any back-flowing from the waste chamber. In addition, an air vent was also located at the end of the waste chamber for reducing the resistance of the flow, when 1 mL of a sample entered the waste chamber. Without this air vent, an overflow of the sample solution into the collection chamber was found.

3.2. Operation of the centrifugal microdevice

The disc operation protocol is shown in Fig. 5. Initially, the lysed sample and the washing solution were orderly flushed into the bead-packed channel at +3500 rpm and were absorbed by SAP in the waste chamber. The bacteria DNA was captured and washed on the surface of the glass beads (Fig. 5a (1)–(3) for schematics & Fig. 5b (2) and (3) for real images). Secondly, the disc was stopped for starting the siphon priming of the elution solution and the LAMP cocktail solution. The siphon priming was proceeded by capillary force of the hydrophilic siphon valve. The speed of −3500 rpm was executed for ejecting the purified captured DNA with the elution solution and the LAMP cocktail/EBT solution into the collection chamber due to the right direction of Coriolis force (Fig. 5a (4) for schematics & Fig. 5b (4) for real image). For enhancing the mixing of the two solutions in the collection chamber, the disc was swirled counter-clockwise and clockwise repeatedly (Fig. 5a (5) for schematics). An additional siphon priming step was applied (Fig. 5a (6) for schematics), and then the disc was spun at −1000 rpm for equally separating the LAMP mixture into 20 aliquots (Fig. 5a (7) for schematics & Fig. 5b (5) for real image). The final step of the spinning program was transferring the 20 aliquots into the individual reaction chamber at −3500 rpm (Fig. 5a (8) for schematics & Fig. 5b (6) for real image). For the LAMP reaction, the Minco heater was maintained at 63 °C, and the disc was moved downward to touch the heater surface. The absorbance intensity at 640 nm (Abs_{640}) and 570 nm (Abs_{570}) was continuously measured for 60 min of the LAMP reaction with an interval of 5 min in all 20 chambers. The ratio of Abs_{640} to Abs_{570} (Abs_{640}/Abs_{570}) was calculated, and then the real-time curve was plotted for the value of Abs_{640}/Abs_{570} ratio versus the reaction time. The overall spinning protocol was shown in Fig. 5b (1) that was programmed in the touch screen of the portable genetic analyzer (Fig. 3a).

3.3. UV–vis absorption measurement of the on-chip LAMP reaction on the portable genetic analyzer

We recorded the UV–vis absorption spectrum of the LAMP mixture before and after LAMP reaction. Before the LAMP reaction, EBT and Mg^{2+} in the LAMP reaction mixture are present in the EBT-Mg complex form, resulting in violet color. If the LAMP reaction proceeds successfully, the released pyrophosphate ions ($P_2O_7^{4-}$) are strongly combined with Mg ions. So, the EBT-Mg complex structure is broken and the EBT^- ion is produced which turns the solution color to sky blue (Fig. S1). Therefore, the color change of the LAMP reaction mixture from violet to sky blue can be used to validate the success of the LAMP reaction (Oh et al., 2016a,b; Rodriguez-Manzano et al., 2016; Wang, 2014). Accordingly, the maximum peak of the absorption wavelength is changed from 570 nm to 640 nm before and after the LAMP reaction (Fig. 6a). Therefore, we designed the UV–vis detector on the portable platform with the two LED light sources with 570 and 640 nm, and the relative absorbance intensities between the two wavelengths (Abs_{640}/Abs_{570}) were calculated and shown in the touch screen. In case of the negative reaction, the absorbance intensity at the wavelength of 570 nm is higher than that of 640 nm (violet line in Fig. 6a), thereby rendering the ratio of Abs_{640}/Abs_{570} less than 1. On the other hand, the positive reaction (blue line in Fig. 6a) displays the ratio of Abs_{640}/Abs_{570} more than 1, because the absorbance intensity at the wavelength of 640 nm is higher than that of 570 nm.

Fig. 6b shows the real-time LAMP profile with 5 min interval on the portable genetic analyzer. The negative control (NC) experiments revealed the constant profile for 60 min of the LAMP reaction, while the positive control (PC) experiment shows a significant change of the Abs_{640}/Abs_{570} ratio round 40-50 min and then a saturation status after 50 min. The ratio of Abs_{640}/Abs_{570} of the PC became higher than 1 when the LAMP product was accumulated. Thus, we could set the Abs_{640}/Abs_{570} value of 1 as the criterion to distinguish the PC from the NC.

3.4. Limit of detection tests on the portable genetic analyzer

We performed the LOD test on the integrated centrifugal microdevice using a portable genetic analyzer. In the 20 reaction chambers, the primer sets targeting pathogenic bacteria were prestored as shown in Fig. 7a. For the LOD test, we utilized the cultured *E. coli* O157:H7 cells with the concentration ranging from 10^2 to 10^5 cells/mL. The color of the reaction chambers (Number #2,6,10,14,18) containing the primer sets for targeting *E. coli* O157:H7 was changed to sky blue, whereas other chambers remained violet, meaning the high specificity of the primers and no cross-contamination between the chambers. Even

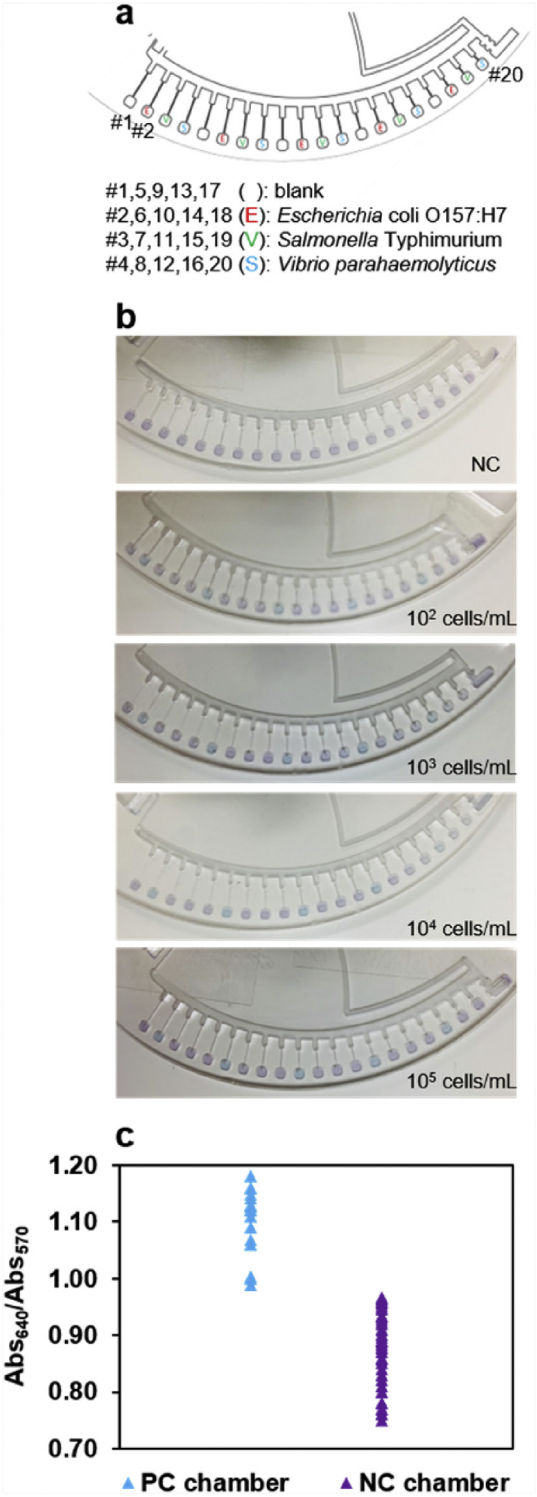

Fig. 7. LOD test on the integrated centrifugal microdevice. (a) 20 reaction chambers were numbered from left to right, and specific primer sets were coated in each reaction chamber. (b) Digital images of the reaction chambers after amplifying fliC gene of *E. coli* O157:H7 with concentrations ranging from 10^2 to 10^5 cells/mL. (c) Analysis of the Abs_{640}/Abs_{570} value for the positive and negative chambers.

with a concentration of 10^2 cells/mL, the reaction chambers amplifying fliC gene of *E. coli* O157:H7 show the color change, demonstrating the low LOD in our proposed system. The colorimetric analysis by naked eyes could mislead us for false-negative or false-positive error. To clarify the positive results, the portable genetic analyzer performed the real-time UV–vis absorption measurement for each chamber and produced the ratio of Abs_{640}/Abs_{570} along the reaction time as described above.

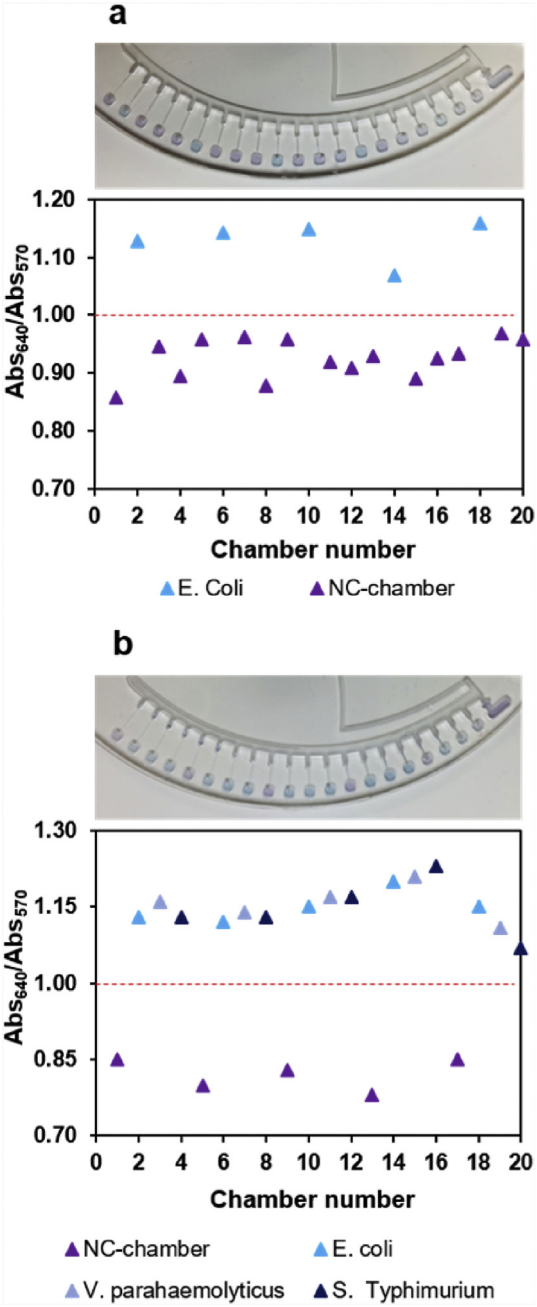

Fig. 8. Multiplex detection of food-borne pathogens on the integrated centrifugal microsystem. (a) (Top) Colorimetric detection for identifying single pathogen (*E. coli* O157:H7) and (Bottom) the graph of the Abs_{640}/Abs_{570} ratio of the 15 negative chambers and 5 positive chambers on the portable genetic analyzer. (b) (Top) Colorimetric detection for identifying three pathogens (*E. coli* O157:H7, *S. Typhimurium* and *V. parahaemolyticus*) and (Bottom) the graph of the Abs_{640}/Abs_{570} ratio of the 5 negative chambers and 15 positive chambers on the portable genetic analyzer.

The value of Abs_{640}/Abs_{570} for the reaction chambers (Number #2,6,10,14,18) was higher than 1, but that of other chambers was lower than 1 (Fig. 7c). These results are in good agreement with the color change of Fig. 7b.

3.5. Monoplex and multiplex analysis for food borne pathogens

The chip was designed for parallel-processing 2 samples in one run and 20 multiplex reaction for each sample. Therefore, theoretically, up to 20 kinds of foodborne pathogens can be simultaneously monitored for one sample. In the multiplex experiment, we targeted three kinds of bacteria (*E. coli* O157:H7, *S. Typhimurium* and *V. parahaemolyticus*) as proof of concept. The experimental procedure is the same as the monoplex detection except that the sample solution contained 10^5 cells/mL of *E. coli* O157:H7, *S. Typhimurium* and *V. parahaemolyticus*. Chambers with air-dried primers for targeting fliC gene of *E. coli* O157:H7 (Number 2,6,10,14,18), invA gene of *S. Typhimurium* (Number 3,7,11,15,19) and toxR gene of V. *parahaemolyticus* (Number 4,8,12,16,20) exhibited a color change from purple into sky blue. No color change was observed in the negative control chambers (Number 1,5,9,13,17) (Fig. 8a). Accordingly, the ratio of Abs_{640}/Abs_{570} was higher than 1.0 in the chambers with positive results, while all the chambers with negative results displayed the value below 1. Consequently, we could demonstrate that the proposed genetic analysis microsystem could simultaneously detect multiplex pathogens with assistance of the optical sensor based on the Abs_{640}/Abs_{570} ratio.

4. Conclusions

In summary, we have demonstrated a sample-to-answer genetic analyzer for multiplex food poisoning bacteria screening with a large volume of sample. The fully integrated centrifugal microdevice was designed with a SAP incorporated waste chamber for a large volume sample treatment and was equipped with a sample loading cartridge for programmed solution injection into the device. In addition, the portable genetic analyzer could perform chip rotation, temperature control, UV–vis absorption for the reaction chamber, and data report. Thus, the whole process for the molecular diagnostics including the solution loading, the DNA extraction, the LAMP reaction, and the optical detection can be processed fully automatically and rapidly with a user-friendly interface, realizing a true POC DNA testing system. Our proposed system could verify three kinds of food borne pathogenic bacteria with LOD of 10^2 cells/mL. We believe that our microsystem makes a great step forward in the fields of point-of-care molecular diagnostics owing to its total integration, automation and high portability.

Declaration of interests

The authors declare that they have no known competing financial interests or personal relationships that could have appeared to influence the work reported in this paper.

Acknowledgments

This work was supported by the Engineering Research Center of Excellence Program of Korea Ministry of Science, ICT & Future Planning (MSIP)/National Research Foundation of Korea (NRF) (2014R1A5A1009799) and by a grant of the Korean Health Technology R&D Project, Ministry of Health & Welfare, Republic of Korea (grant no. HI13C1232).

Appendix A. Supplementary data

Supplementary data to this article can be found online at https://doi.org/10.1016/j.bios.2019.04.035.

References

Andreasen, S.Z., Kwasny, D., Amato, L., Brøgger, A.L., Bosco, F.G., Andersen, K.B., Svendsen, W.E., Boisen, A., 2015. RSC Adv. 22, 17187–17193.
Antillon, M., Saad, N.J., Baker, S., Pollard, A.J., Pitzer, V.E., 2018. J. Infect. Dis. S255–S267.
Berg, B., Cortazar, B., Tseng, D., Ozkan, H., Feng, S., Wei, Q., Chan, R.Y.-L., Burbano, J., Farooqui, Q., Lewinski, M., Di Carlo, D., Garner, O.B., Ozcan, A., 2015. ACS Nano 8, 7857–7866.
Choi, G., Jung, J.H., Park, B.H., Oh, S.J., Seo, J.H., Choi, J.S., Kim, D.H., Seo, T.S., 2016. Lab Chip 12, 2309–2316.
Choi, G., Prince, T., Miao, J., Cui, L., Guan, W., 2018. Biosens. Bioelectron. 115, 83–90.
Choi, J.R., Tang, R., Wang, S., Wan Abas, W.A.B., Pingguan-Murphy, B., Xu, F., 2015. Biosens. Bioelectron. 74, 427–439.
Choi, J.R., Yong, K.W., Tang, R., Gong, Y., Wen, T., Li, F., Pingguan-Murphy, B., Bai, D., Xu, F., 2017a. Trends Anal. Chem. 93, 37–50.
Choi, S., Hwang, J., Lee, S., Lim, D.W., Joo, H., Choo, J., 2017b. Sens. Actuators, B 240, 358–364.
Deng, X., Wang, C., Gao, Y., Li, J., Wen, W., Zhang, X., Wang, S., 2018. Biosens. Bioelectron. 105, 211–217.
DuVall, J.A., Le Roux, D., Thompson, B.L., Birch, C., Nelson, D.A., Li, J., Mills, D.L., Tsuei, A.-c., Ensenberger, M.G., Sprecher, C., Storts, D.R., Root, B.E., Landers, J.P., 2017. Anal. Chim. Acta 980, 41–49.
Hoffmann, J., Mark, D., Lutz, S., Zengerle, R., von Stetten, F., 2010. Lab Chip 11, 1480–1484.
Jung, J.H., Park, B.H., Choi, Y.K., Seo, T.S., 2013. Lab Chip 17, 3383–3388.
Jung, J.H., Park, B.H., Oh, S.J., Choi, G., Seo, T.S., 2015. Biosens. Bioelectron. 68, 218–224.
Kim, T.-H., Kim, C.-J., Kim, Y., Cho, Y.-K., 2018. Sens. Actuators, B 256, 310–317.
Liu, Q., Zhang, X., Chen, L., Yao, Y., Ke, S., Zhao, W., Yang, Z., Sui, G., 2018. Sens. Actuators, B 270, 371–381.
Loonen, A.J.M., Bos, M.P., van Meerbergen, B., Neerken, S., Catsburg, A., Dobbelaer, I., Penterman, R., Maertens, G., van de Wiel, P., Savelkoul, P., van den Brule, A.J.C., 2013. PLoS One 8, e72349.
Martin, J.W., Nieuwoudt, M.K., Vargas, M.J.T., Bodley, O.L.C., Yohendiran, T.S., Oosterbeek, R.N., Williams, D.E., Cather Simpson, M., 2017. Analyst 10, 1682–1688.
Oh, S.J., Park, B.H., Choi, G., Seo, J.H., Jung, J.H., Choi, J.S., Kim, D.H., Seo, T.S., 2016a. Lab Chip 10, 1917–1926.
Oh, S.J., Park, B.H., Jung, J.H., Choi, G., Lee, D.C., Kim, D.H., Seo, Tae S., 2016b. Biosens. Bioelectron. 75, 293–300.
Park, B.H., Oh, S.J., Jung, J.H., Choi, G., Seo, J.H., Kim, D.H., Lee, E.Y., Seo, T.S., 2017. Biosens. Bioelectron. 91, 334–340.
Priye, A., Wong, S., Bi, Y., Carpio, M., Chang, J., Coen, M., Cope, D., Harris, J., Johnson, J., Keller, A., Lim, R., Lu, S., Millard, A., Pangelinan, A., Patel, N., Smith, L., Chan, K., Ugaz, V.M., 2016. Anal. Chem. 9, 4651–4660.
Rodriguez-Manzano, J., Karymov, M.A., Begolo, S., Selck, D.A., Zhukov, D.V., Jue, E., Ismagilov, R.F., 2016. ACS Nano 3, 3102–3113.
Schwemmer, F., Blanchet, C.E., Spilotros, A., Kosse, D., Zehnle, S., Mertens, H.D.T., Graewert, M.A., Rössle, M., Paust, N., Svergun, D.I., von Stetten, F., Zengerle, R., Mark, D., 2016. Lab Chip 7, 1161–1170.
Stedtfeld, R.D., Tourlousse, D.M., Seyrig, G., Stedtfeld, T.M., Kronlein, M., Price, S., Ahmad, F., Gulari, E., Tiedje, J.M., Hashsham, S.A., 2012. Lab Chip 8, 1454–1462.
Stumpf, F., Schwemmer, F., Hutzenlaub, T., Baumann, D., Strohmeier, O., Dingemanns, G., Simons, G., Sager, C., Plobner, L., von Stetten, F., Zengerle, R., Mark, D., 2016. Lab Chip 1, 199–207.
Takalkar, S., Baryeh, K., Liu, G., 2017. Biosens. Bioelectron. 98, 147–154.
van Oordt, T., Barb, Y., Smetana, J., Zengerle, R., von Stetten, F., 2013. Lab Chip 15, 2888–2892.
Wang, D.G., 2014. Appl. Mech. Rev. 618, 264–267.
Wang, L.-J., Chang, Y.-C., Sun, R., Li, L., 2017. Biosens. Bioelectron. 87, 686–692.
Ye, X., Xu, J., Lu, L., Li, X., Fang, X., Kong, J., 2018. Anal. Chim. Acta 1018, 78–85.
Zhang, L., Ding, B., Chen, Q., Feng, Q., Lin, L., Sun, J., 2017. Trends Anal. Chem. 94, 106–116.
Zhao, Y., Czilwik, G., Klein, V., Mitsakakis, K., Zengerle, R., Paust, N., 2017. Lab Chip 9, 1666–1677.